*Journal of Basic Physical Research ISSN: 2141-8403 Prints, 2141-8411 Online*
*Vol.13, August, 2024, pp. 76 – 90, Available online at www.jbasicphyres-unizik.org*

# USING EULER DECONVOLUTION AND SOURCE PARAMETER IMAGING (SPI) OF GRAVITY DATA FOR DEPTH-TO-BASEMENT DETERMINATION IN PARTS OF SOUTHEASTERN NIGERIA

**[1]Umeh M. C., [2]Obiekezie T. N. and [3]Akiang F. B.**
*[1]Department of Applied Geophysics, Nnamdi Azikiwe University, Awka, Nigeria.*
*[2]Department of Physics and Industrial Physics, Nnamdi Azikiwe University, Awka, Nigeria.*
*[3]Department of Geology, Federal University of Technology, Owerri, Nigeria.*
*Corresponding author: mc.umeh@unizik.edu.ng*

***Abstract***
*Ground gravity data were interpreted in parts of Southeastern Nigeria using Euler deconvolution. This study estimates the depth of basement rocks and identifies possible geological and geophysical features. The study area is between longitude $7^0$E to $8^0$E and latitude $5^0$30'N to $6^0$30'N within the Southeastern part of Nigeria and covers aspects of Enugu, Ebonyi, Anambra, Abia, Imo, and Cross River State. The digitized data from the Nigerian Geological Survey Agency (NGSA) by Ground Survey were processed and interpreted to get the basement's depth in Southeastern Nigeria. The Bouguer gravity data imported from the Microsoft Excel spreadsheet into Geosoft were gridded using the miniature curvature interface and then residualized. The separation of the regional and residual anomalies followed this. The Bouguer gravity anomaly grid, the regional grid, and the residual grid were all reprojected from geographical coordinates (Latitude and Longitude) to the Universal Transverse Mercator (UTM) in meters. The interpretation of gravity data using Euler deconvolution was used to specify the Structural Index (SI). The results indicate that contact faults can be interpreted with an SI of 0.0, while dyke or sill with an SI of 1.0. The scattered Euler deconvolution solution suggests that the intrusive body extends well beyond the study area. The result reveals that the fault, though more than one on the surface in the study area, trends NE – SW. The estimated depth to the basement ranges from 3584.9 m to 7992 m. The SPI data show a minimum depth of 237.49m and a maximum depth of 82748.37m, with an average depth of 3100.174m, but the actual value, as shown on the grid map, is 12678.8 m for the most profound source to the basement and 398.5 m for the shallowest source to the basement. This depth range and fault observed could influence the accumulation of minerals and hydrocarbon in the study area.*
***Keywords:*** *Bouguer gravity, Basement, Residual Anomaly, Euler Deconvolution, Source Parameter Imaging, Estimated Depth.*

## Introduction

Variations in the density and porosity of the subterranean rocks result in changes to the gravity fields. Gravity surveying is also helpful in searching for intrusive bodies and significant faults. Gravity data has many applications and can yield beneficial subsurface information (Okwesili *et al.*, 2020).

The gravity survey method is greatly helpful in searching for intrusive bodies and prominent faults. Euler deconvolution and source parameter imaging are simple techniques for interpreting gravity data to improve output results and help an explorer understand. Euler deconvolution technique has become broadly used to analyze profile or girded gravity survey data. This technique provides automatic estimates of source location and depth. Therefore, Euler deconvolution is both a boundary finder and a depth estimation. With the help of a structural index, Euler deconvolution plays a significant role in gaining a better understanding of thrust-fault delineation and provides a mappable solution (Ghosh, 2022). The derived values shown in Table 1.1 is from Reid *et al*., (1990). In addition, the value of the SI plays a vital role in this technique because the use of the wrong values leads to the interpretation of misleading depths.

The accuracy of the source parameter imaging is similar to that of Euler deconvolution. However, SPI has the advantage of producing a complete set of coherent solution points, making it easier to use. One of the stated objectives of the SPI approach is for a local

geology expert to be able to analyze the produced pictures quickly (Thurston & Smith,1997; Ahmed & Alaa, 2019).

Identifying trends and depths are the most significant outcomes of Euler deconvolution. The choice of a structural index (SI) is the primary determinant of the quality of depth estimate using Euler deconvolution. Furthermore, magnetic data can benefit from the application of Euler deconvolution but when compared to the magnetic survey data, the gravity is more intricate.

This work intends to produce the regional and residual anomaly maps and determine the depth of the gravity sources and the area's basement using Euler deconvolution and Source parameter imaging.

*Location of the Study Area*




*Fig 1: Map of Nigeria showing Study Area.*

The study area falls within the Southeastern part of Nigeria (Fig. 1), occupying portions of Enugu, Ebonyi, Anambra, Abia, Imo, and Cross River State. The study area is located between longitude $7^0$E to $8^0$E and latitude $5^0$30'N to $6^0$30'N (Fig. 2). The study area has gravity Bouguer anomaly maps and a total of 110.57 x 110.57 square kilometer (~111x111 square kilometer), which are part of the standard half degree by half degree ($1/2^0$) Nigerian Geological Survey Agency (NGSA) 1: 250,000 scale.

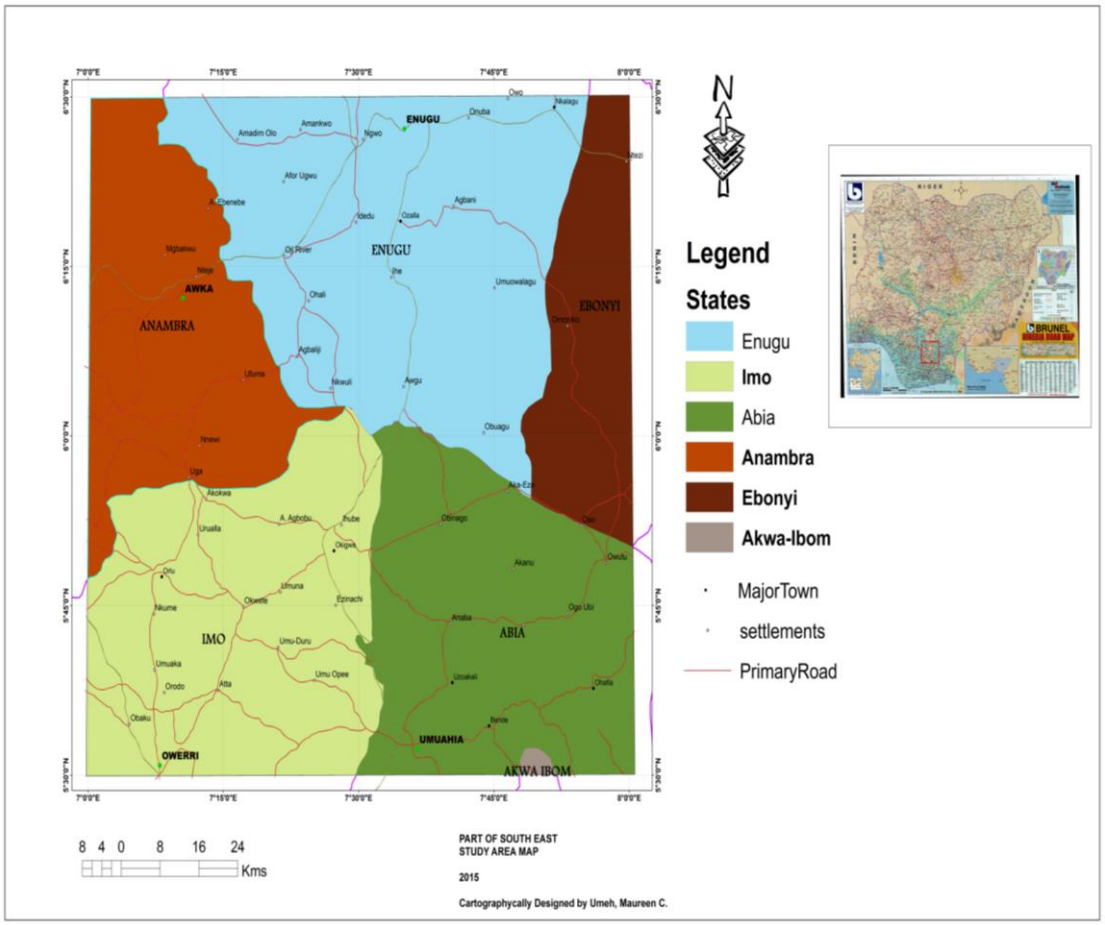



*Fig 2: Map of Study Area.*

**Regional Geology of the Study Area**

The Study Area is located within the southern part of the Anambra Basin and a portion of the Northern part of the Niger Delta Complex. Therefore, the primarily exposed lithologies are Cretaceous sandstones, shale and siltstones, Tertiary clay, sandstones, and shales (Fig 3).

Most of the mineral prospects are related to the extensive sedimentary sequence within both the Anambra and Niger Delta basins: clay on coastal plain sands and river channels; coal along the Benue-Anambra basins border, flat-lying at the base of the escarpment (steep-slope); brine on shale and sand sequences; lead/zinc on shale and siltstones; limestones on alternating series of shales, limestones, mudstones and sandstones (NGSA, 2006).

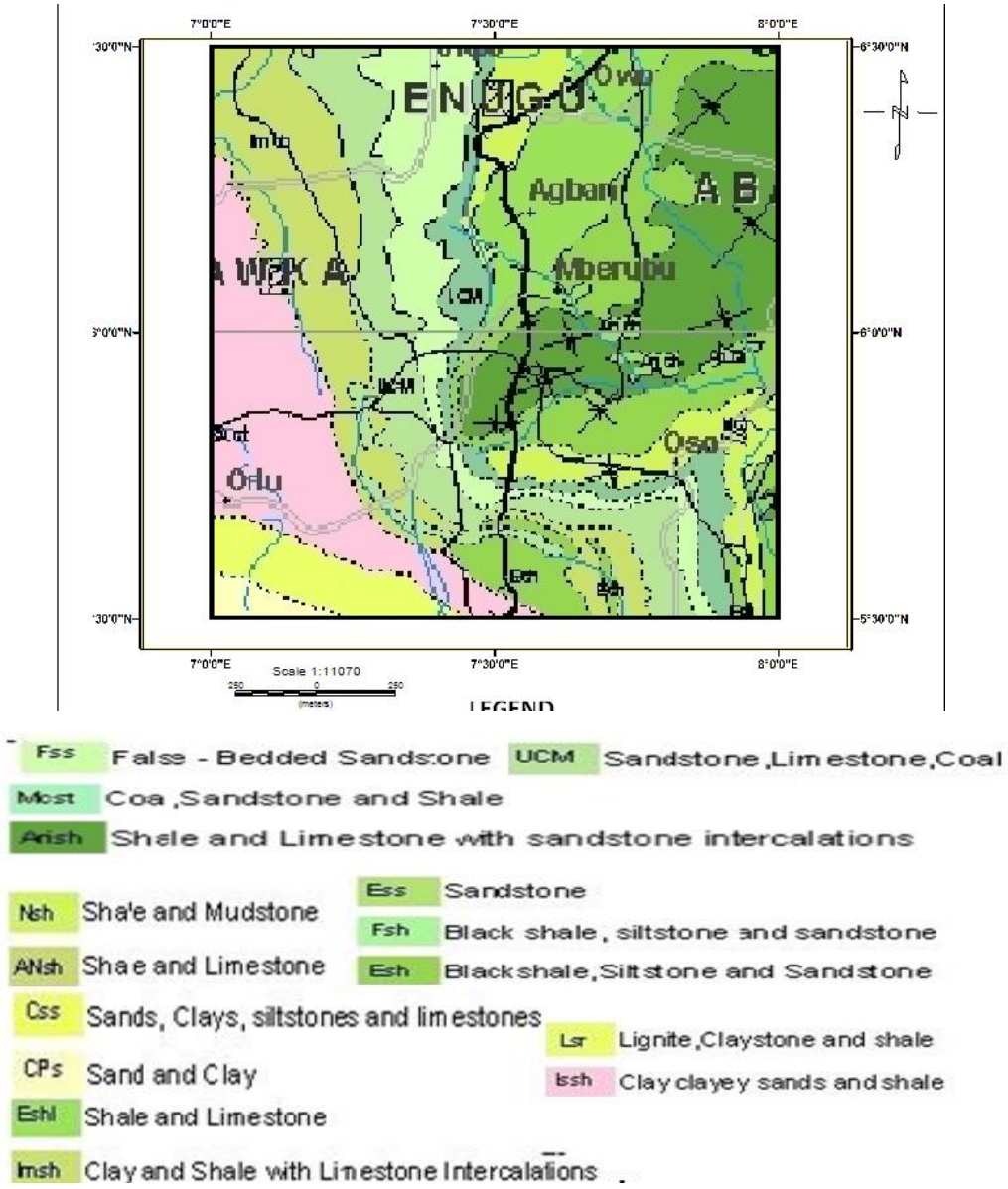



*Fig 3: Geological map of the Study Area.*

## Methodology

The Nigerian Geological Survey Agency carried out the ground survey in southeastern Nigeria. The Bouguer gravity anomaly grid, the regional grid, and the residual grid were all re-projected from the Geographic coordinate system (Longitude/Latitude) to UTM (in meters) to calculate depth. The Station densities were Ebonyi 1/11 km2, Enugu 1/8 km2, and Anambra 1/6.7 $km^2$.

## Data Processing

Bouguer gravity anomaly and Shuttle Radar Topography Mission (SRTM) for elevation gridded maps of the survey area were produced using the Geosoft software, Surfer 10 was used for contouring, and ArcGIS was used for producing a map of the study area. Regional and residual separation was carried out using the Bouguer gravity data. This was done by subtracting continued data of the Bouguer gravity upward to 2 km from the regional gravity

data (low pass filter) to obtain a gravity response from the earth's upper crust comprising the basement and the sedimentary units.

*Euler Deconvolution***:** The Standard Euler Deconvolution was performed on the gravity data. The physically plausible Structural Index values range from -1 to 2 (Table 1). Field strength or SI values imply that it increases with distance from the source.

**Table 1: Structural index for gravity (FitzGeralda *et al*., 2004)**

| ***Source*** | ***SI*** |
|---|---|
| Sphere | 2 |
| Horizontal Cylinder features | 1 |
| Fault (small step) | 0 |
| Contact | -1 |

The Euler depth solutions were obtained using a Structural Index of 0.0 and 1.0. Window Size was varied between 15 and 20 while the Maximum Percentage Tolerance of 5, 10, and 20 were used. These parameters yielded the most consistent solutions after trials with several different values. The Euler Deconvolution process required partial derivatives of the input grid.

The size of the Euler window influenced the maximum depth for Euler solutions. The size of the Euler window is directly related to the maximum depth of solutions. The window size determines the number of observations to pass to the solver for the current point of interest in the grid.

The two-dimensional form of Euler deconvolution for a homogeneous anomaly field $f$ measured at a location $(x, z)$ is

$$\frac{\partial f}{\partial x}(x - x_0) + \frac{\partial f}{\partial x}(z - z_0) = SI.f \ldots\ldots\ldots\ldots\ldots\ldots\ldots\ldots\ldots\ldots\ldots (1)$$

where the source location and depth are $(x_0, z_0)$ (Thompson, 1982).

Applying Euler deconvolution to the vertical gradient of the gravity or magnetic field provides improved source resolution:

$$\frac{\partial}{\partial x}\left(\frac{\partial^n f}{\partial z^n}\right)(x - x_0) + \frac{\partial}{\partial z}\left(\frac{\partial^n f}{\partial z^n}\right)(z - z_0) = -(SI + n)\left(\frac{\partial^n f}{\partial z^n}\right) \ldots\ldots\ldots\ldots\ldots\ldots (2)$$

As stated in the following sources: Hsu, 2002; Ravat *et al*., 2002; Cooper and Cowan, 2003. where n is the order of the gradient employed, which need not be an integer. It may be used on the horizontal gradient in a similar way.

$$\frac{\partial}{\partial x}\left(\frac{\partial^n f}{\partial x^n}\right)(x - x_0) + \frac{\partial}{\partial z}\left(\frac{\partial^n f}{\partial x_n}\right)(z - z_0) = -(SI + n)\left(\frac{\partial^n f}{\partial x^n}\right) \ldots\ldots\ldots\ldots\ldots (3)$$

(Huang *et al*., 1995).

In different geological formations, the Euler depths reflect differences in structure and/or stratigraphy. Consequently, Euler solutions arise in the research areas geological formations whenever lithologic discontinuities are present.

**Results and Discussion**

Fig 4 is the Bouguer anomaly grid of the study area showing gravity high trending NE – SW at the center with negative gravity on the NW and the SE ends. These three distinctive areas: clearly indicates change in density from a high Bouguer anomaly in the middle being bounded by gravity lows at the sides.

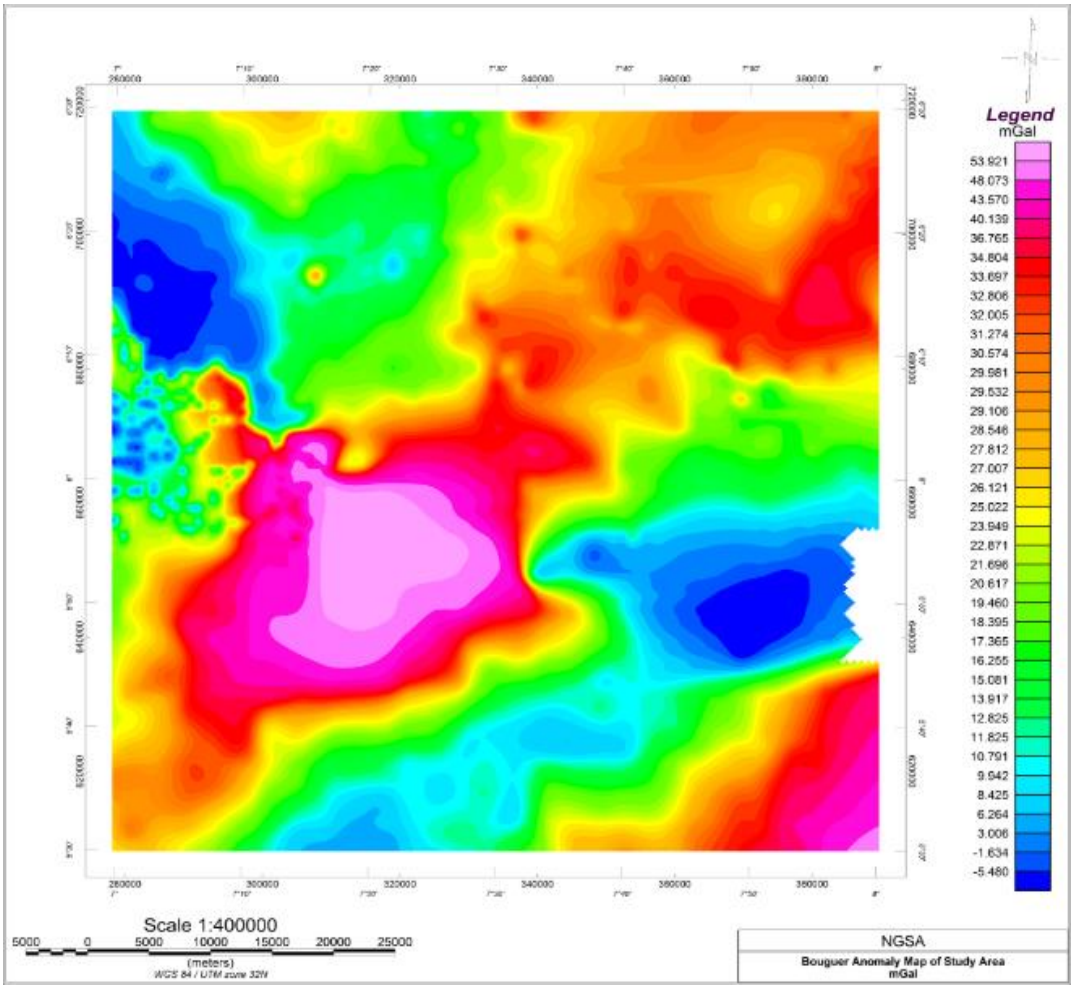



*Fig 4: The Gravity Bouguer anomaly map of the study area obtained using Oasis Montaj.*

The gravity anomaly map in Fig 5 is characterized by circular contours, while some contours are elliptical with well-defined trends and have tectonic implications. The gravity field has distinct gradients.

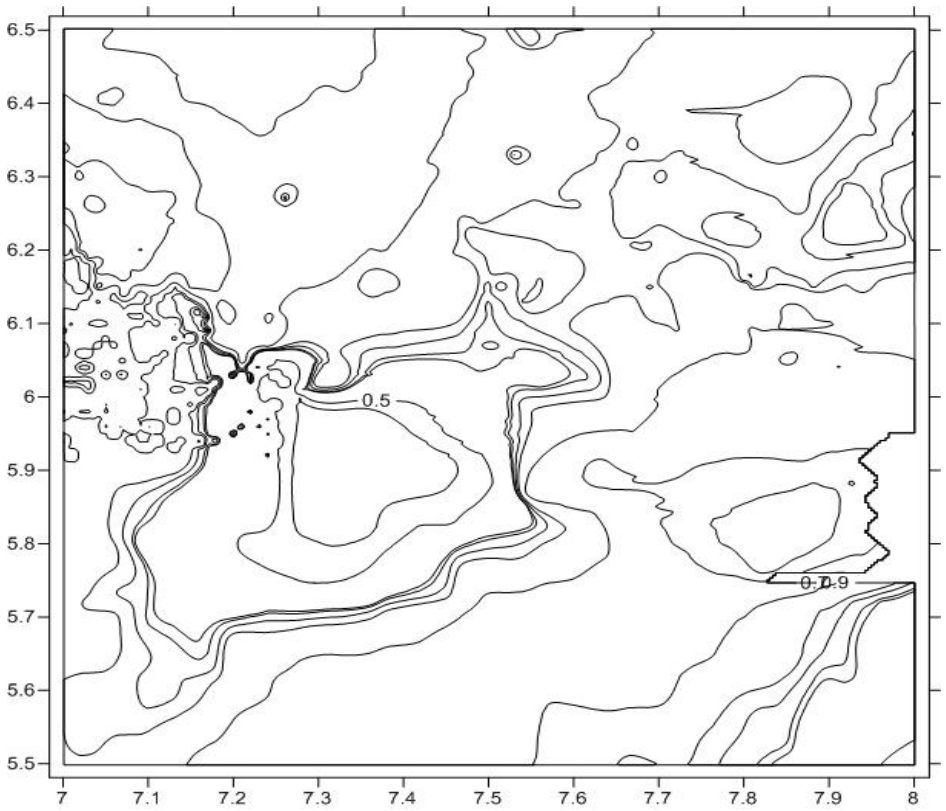



*Fig 5: Gravity Bouguer Anomaly Map of study Area obtained using surfer 10.*

The residual (high-pass filter) anomalies and the regional (low-pass filter) background field must be distinguished for accurate interpretation. Numerous local abnormalities are visible on the residual map (Fig. 6). Localities with positive residual anomalies suggest either basement uplift or a lateral difference in density from the causing rocks. The deeper heterogeneity of the earth's crust is primarily responsible for the more prominent characteristics, which appear as trends across a significant distance. The principal interest is on the more minor local disturbances that sometimes skew these patterns, referred to as regional. The more minor, more localized disruptions are referred to as residual anomalies, and they may offer proof of the presence of bodies or structures with various densities.

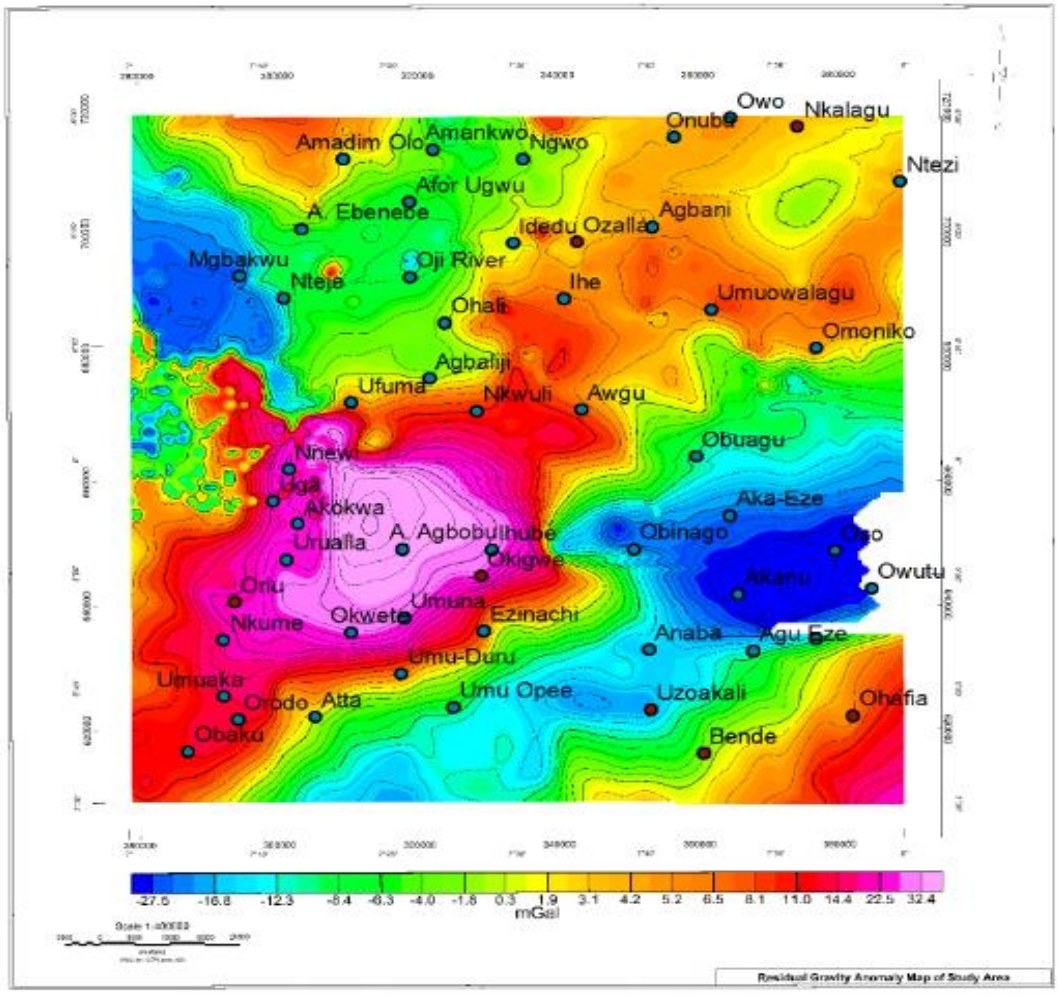



*Fig 6: Residual Gravity Bouguer Anomaly Map of Study Area*

**Derivatives**

The analysis that produces the contact parameters for the Euler deconvolution and Source parameter imaging in this instance covers both the horizontal components (dx, dy) and vertical components (dz). These derivatives are frequently employed in prospecting to characterize several shallow bodies in an area. Shallow bodies are defined in the regions by derivatives (Fig.7) of the gravity field, which reduce low-frequency components and augment high-frequency components.

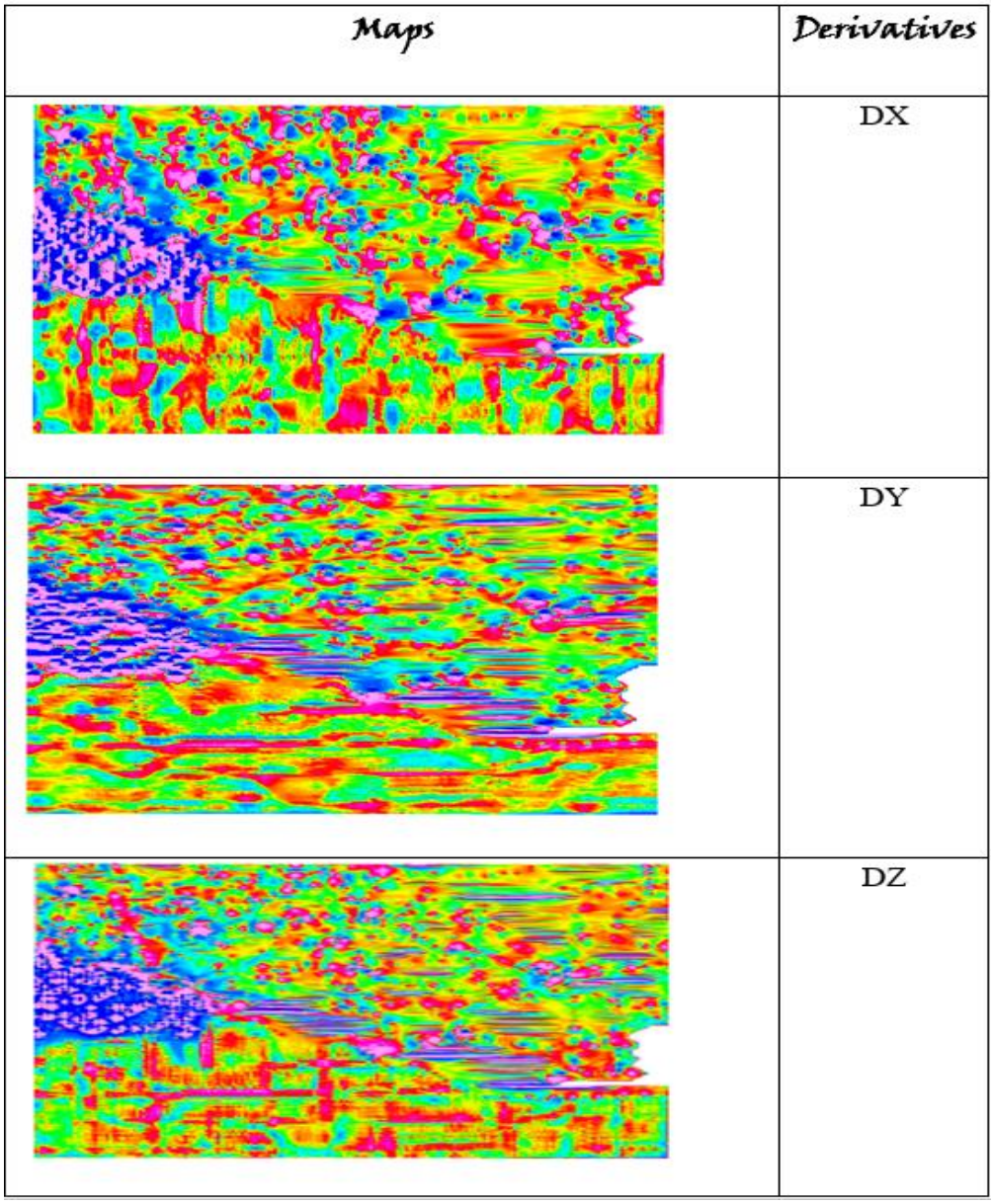



*Fig 7: Derivatives used for plotting the depth solution maps.*

**Euler Deconvolution Depth Estimation**

Euler Deconvolution calculates location, depth below sensor and reliability for each solution as well as error estimates in the form of standard deviations. The primary signal that is measured is derived from the edges or contacts of geological units. The inferred source parameters following the baselines described in the methodology, the local depth (Horizontal Cylinder and Fault), plotted by performing Euler deconvolution on the residual Bouguer data in an attempt to find depth to basement with structural index 0.0 (Fig 8 and 9) to locate contact/faults and index 1.0 (Fig 10 and 11) to locate horizontal features. The derivatives (DX, DY and DZ) in Fig 7 were used.

Two maps were plotted for both S.I = 0.0 (Fig 8 and 9) and S.I = 1.0 (Fig 10 and 11) respectively by varying the percentage depth tolerance and window size to get suitable maps. The faults are located at 3584.9 m and 3420.2 m while the horizontal features lie at the depth of about 7992.0 m and 7943.4 m.

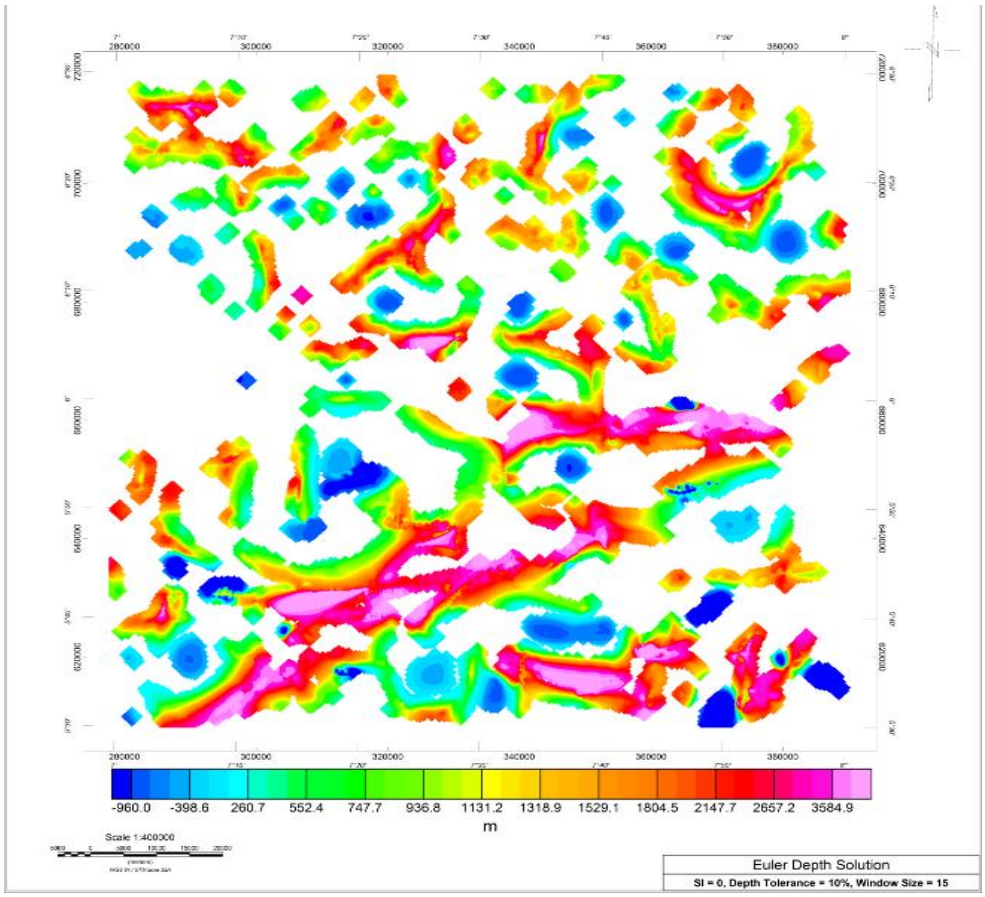



*Fig 8: Euler depth solution map (for SI = 0, % Tolerance = 10%, Window Size = 15).*

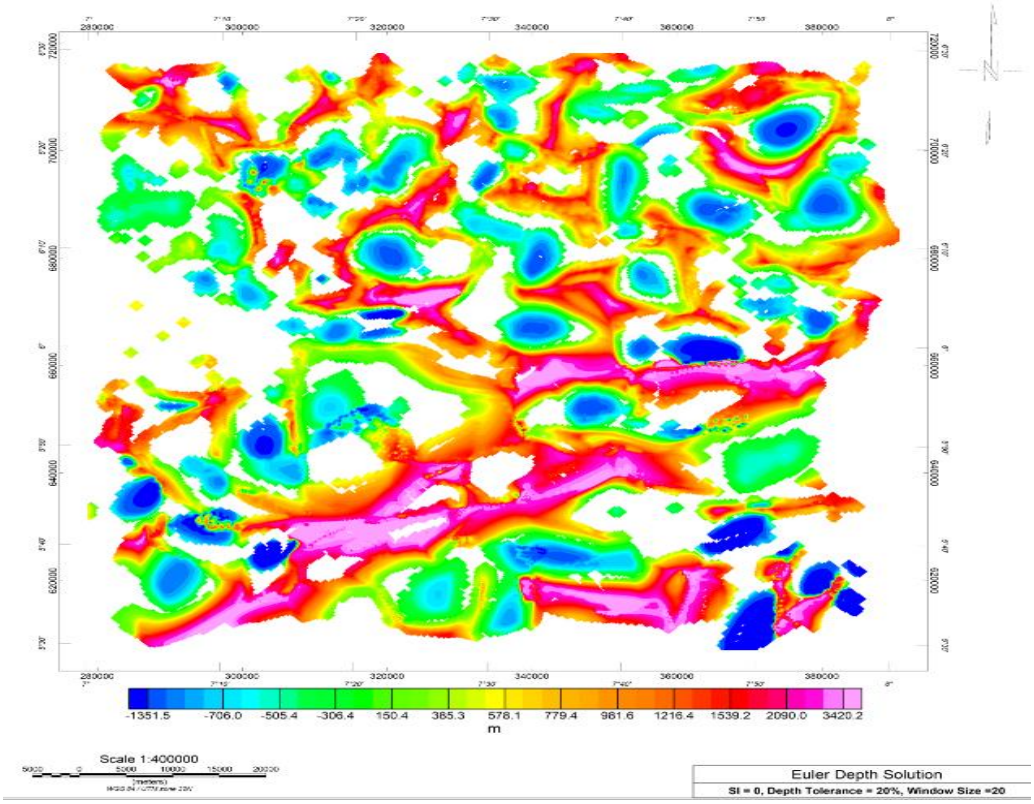



*Fig 9: Euler depth solution map (for SI = 0.0, % Tolerance =20, Window Size = 20).*

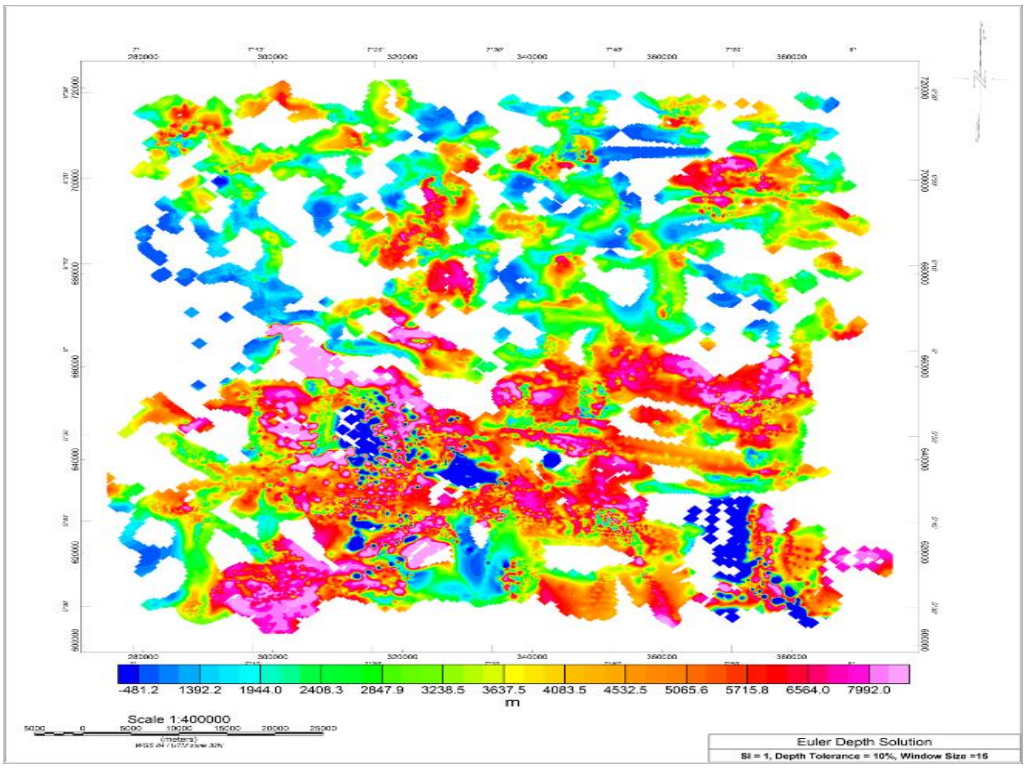



Fig 10: Euler depth solution map (for SI = 1.0, % Tolerance =10, Window Size = 15).

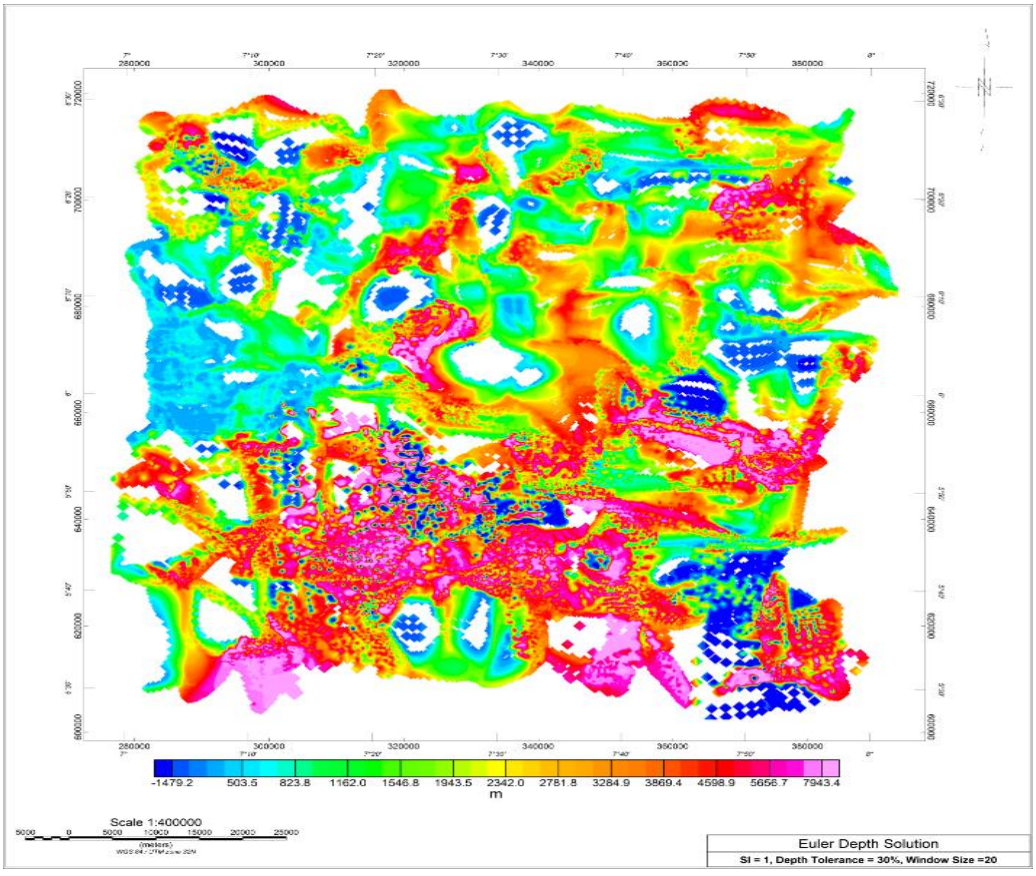



*Fig 11: Euler depth solution map (for SI = 1.0, Window Size = 10, Depth Tolerance = 30%).*

The results show that simple gravity features from the calculated Euler deconvolution maps trend to estimate the depths of the actual bodies. Thus, when the Euler deconvolution is applied to the residual gravity data (Fig 6), it would typically expect depth estimates to be slightly shallower and more accurate on the data. The scattered Euler deconvolution solution confirms that the intrusive body extends well beyond the study area. The absence of such scattered solutions in some parts of the areas suggests that the intrusive body is not confined to all parts of the survey area (as shown in Fig 8, Fig 9, Fig 10, and Fig. 11). There is one significant fault contact from the Euler solution on the image of Fig 8 and Fig 9; the fault, though more than one on the surface in the study area, trends NE - SW. This agrees with the observations of Benkhelil *et al*. (1998) that there are major NE-SW lineaments in the sedimentary basins and the basement complex of South to Northeast Nigeria. In some cases, the lack of Euler solutions may be due to minor faults having little to no gravity contrast between sediments filled in with faults and surrounding lithologies. The horizontal features in Fig 8 and 9 are high at the southern part of both maps.

The mean maximum and minimum for SI (0) are 9720.69 m and -3271.76 m, while the actual maximum value is 3584.9 m, and SI (1) has a maximum and minimum of 19582.75 m and -11554.28 m, respectively, with an actual maximum value of 7992 m. Therefore, Euler deconvolution is remarkably suggested for examining large data sets. The alignment of consistent clusters of Euler depth solutions at all depths suggests that the lineaments permeate the sedimentary section above the basement.

**Depth Estimation using Source Parameter Imaging (SPI)**

Figure 12 shows the depth estimate of the upper basement depth (i.e. top of the sediment/basement interface). The white areas/portions of Figure 13 are the areas where the derivative used to estimate the local wave number are so small that the SPI structural index cannot be estimated reliably. The Source Parameter Imaging (SPI) module from Oasis Montaj software was applied to the Bouguer data of the study area. The model-independent local wave number had been set to zero in that portion. From Figure 12, the depth to sedimentary/basement interface varies. The SPI statistics shows a minimum depth of 237.49m and a maximum depth of 82748.37m with an average of 3100.174m while the true value as on the grid map is 12678.8 m for the deepest source to the basement and 398.5 m for the shallowest source to basement.

Depth to basement Profile map (Fig 12) show that the deepest part of the basin coincided with those obtained from the modelling. The highest depth can be mainly found at the south-central part (around the Okigwe Area) and scattered little at the other ends while the shallowest depths can be found at the north to the western part.

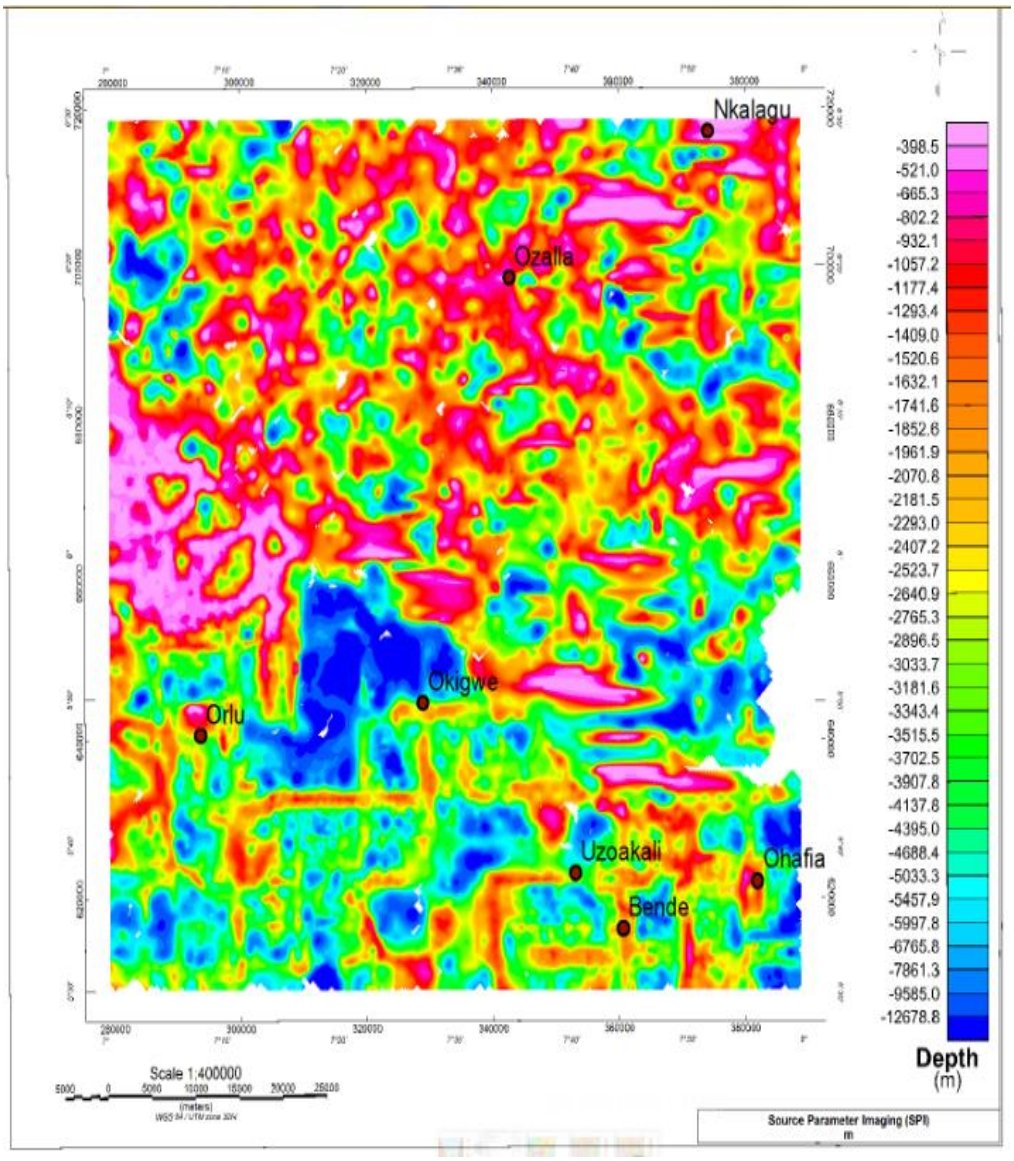



*Fig 12: Depth determination from source parameter imaging (SPI). The colour bar shows the depth estimates in meter.*

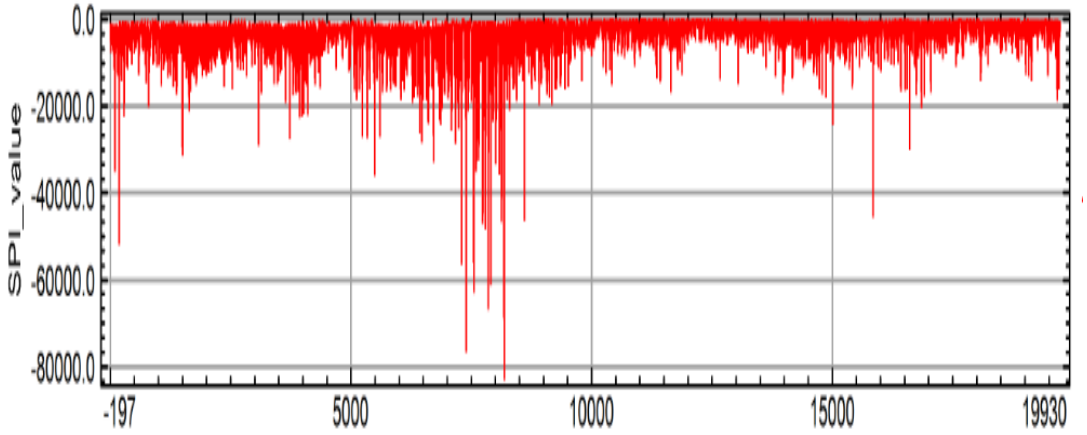



*Fig 13: Source Parameter Imaging Depth Profile Map of the Study Area.*

## Conclusion

The Bouguer gravity data and residual map revealed a linear depression with sediment accumulation trending NE-SW in the study area. The correspondence of Euler deconvolution results at the study area in the gravity image suggests that the Euler deconvolution technique can be used to extend the knowledge of faulting and buried body underneath ground surface. A lack of contrast in gravity properties of materials juxtaposed at the fault or minor offs*et al*ong the fault can cause unable detection in Euler deconvolution. Also, the structure index of 0.0 for a simple gravity body can be used to reveal a boundary of fault contact and lithology boundaries.

The real contact faults are typically complex structures, so that some geological features cannot be detected by Euler deconvolution technique.

## Acknowledgment

Sincerely grateful to the Nigerian Geological Survey Agency, Abuja for providing the data used for this work.

## Reference

Al-Banna, A. & Daham, Alaa., (2019). Application of Source Parameter Imaging (SPI) Technique to Gravity and Magnetic Data to Estimate the Basement Depth in Diyala Area, Eastern Central Iraq. . Iraqi Journal of Science. 60. 601-609. 10.24996/ijs.2019.60.3.18.

Benkhelil, J., Mascle, J. & Guiraud, M., (1998). Sedimentary and structural characteristics of the Cretaceous Cote D' Ivoire- Ghana Transform Margin and in the Benue Trough: A comparison. In: Proceedings of the Ocean Drilling Program, Scientific Results, 159, 93 - 99.

Cooper, G. R. J., & Cowan, D. R., (2003). Applications of fractional calculus to potential field data. Exploration Geophysics, 34, 51–56.

FitzGerald, D., Reid, A. & McInerney, P. (2004). New discrimination techniques for Euler deconvolution. Computers & Geosciences, . 30, 461–469.

Ghosh, G. K., (2022). Delineation of major subsurface structural features and source depth locations using 3-D Euler deconvolution of gravity data at the north-eastern part of India. Acta Geophys. 70, 2033–2044.

Huang, D., Gubbins, D., Clark, R.A., & Whaler, K.A., (1995). Combined study of Euler's homogeneity equation for gravity and magnetic field. In 57th EAGE Conference and Technical Exhibition, Extended abstracts, 144, DOI: 10.3997/2214-4609.201409565

Hsu, S. K., (2002). *Imaging magnetic sources using Euler's equation.* Geophysics. Prospecting, 50, 15-25.

Okwesili, N. A., Okeke, F. N. & Orji, P. O. (2020). Geophysical survey of aerogravity anomalies over Lafia and Akiri regions of middle Benue trough, Nigeria, employing

Power Spectrum and Source Parameter Imaging technique. IOSR Journal of Applied Physics (IOSR-JAP), 12(5), 2020, . 58-68.

Ravat, D., Kirkham, K., & Hildenbrand, T.G., (2002). A source-depth separation filter: Using the Euler method on the derivatives of total intensity magnetic anomaly data. The Leading Edge, 21, 360–365.

Reid, A. B., Allsop, J. M., Granser, H., Millet, A. J., & Somerton, I. W. (1990), Magnetic interpretation in three dimensions using Euler deconvolution. Geophys. 55, 80–91.

Thompson, D. T., (1982). EULDPH: A new technique for making computer-assisted depth estimates from magnetic data. Geophysics. 47, 31–37.

Thurston, J.B. & Smith, R.S. (1997). Automatic conversion of magnetic data to depth, dip, and susceptibility contrast using the SPI ™ method: Geophysics, 62: 807-813.